

System Level Synchronization of Phase-Coded FMCW Automotive Radars for RadCom

Lampel, Franz; Uysal, Faruk; Tigrek, Firat; Orru, Simone; Alvarado, Alex; Willems, Frans; Yarovoy, Alexander

DOI

[10.23919/EuCAP48036.2020.9135417](https://doi.org/10.23919/EuCAP48036.2020.9135417)

Publication date

2020

Document Version

Final published version

Published in

14th European Conference on Antennas and Propagation, EuCAP 2020

Citation (APA)

Lampel, F., Uysal, F., Tigrek, F., Orru, S., Alvarado, A., Willems, F., & Yarovoy, A. (2020). System Level Synchronization of Phase-Coded FMCW Automotive Radars for RadCom. In *14th European Conference on Antennas and Propagation, EuCAP 2020* Article 9135417 (14th European Conference on Antennas and Propagation, EuCAP 2020). IEEE. <https://doi.org/10.23919/EuCAP48036.2020.9135417>

Important note

To cite this publication, please use the final published version (if applicable). Please check the document version above.

Copyright

Other than for strictly personal use, it is not permitted to download, forward or distribute the text or part of it, without the consent of the author(s) and/or copyright holder(s), unless the work is under an open content license such as Creative Commons.

Takedown policy

Please contact us and provide details if you believe this document breaches copyrights. We will remove access to the work immediately and investigate your claim.

Green Open Access added to TU Delft Institutional Repository

'You share, we take care!' - Taverne project

<https://www.openaccess.nl/en/you-share-we-take-care>

Otherwise as indicated in the copyright section: the publisher is the copyright holder of this work and the author uses the Dutch legislation to make this work public.

System Level Synchronization of Phase-Coded FMCW Automotive Radars for RadCom

Franz Lampel*, Faruk Uysal[†], Firat Tigrek*, Simone Orru[†], Alex Alvarado*, Frans Willems*, Alexander Yarovoy[†]

*Eindhoven Univ. of Technology, Eindhoven, The Netherlands, {f.lampel, r.f.tigrek, a.alvarado, f.m.j.willems}@tue.nl

[†]Delft University of Technology, Delft, The Netherlands, {f.uysal, a.yarovoy}@tudelft.nl

Abstract—This paper describes an FMCW based radar and communication (RadCom) system and addresses the challenges in the synchronization of multiple units for communication functionality. We proposed a novel technique to detect the FMCW RadCom signal at the communication receiver and derive the detection and false alarm probabilities of it. Moreover, to achieve fine synchronization between transmit and receive devices, a novel approach based on FMCW RadCom signal time of arrival estimation is proposed. The potential capability of a RadCom system is experimentally demonstrated for the first time by a set of automotive-grade mmWave radars with GPS-based synchronization.

Index Terms—phase-coded radar, PC-FMCW, RadCom, Joint sensing and communication

I. INTRODUCTION

Building situational awareness for autonomous vehicles is currently addressed by adding multiple sensors (including radars) on board as well as providing communication links with other vehicles and road infrastructure. A use case where vehicle-to-vehicle (V2V) communication is indispensable is driving as part of a group of vehicles, which is termed as platooning. Both the operation of multiple radars and V2V communication involving multitudes of vehicles put a strain on the available spectrum resources. Combining radar and communication functions by modulating the radar signal with communication payload is considered in previous publications, where frequency modulated continuous wave (FMCW) radar signals are phase modulated for joint radar communication (RadCom) applications [1], [2]. While previous research focuses on the investigation of phase-coded FMCW (PC-FMCW) radar performance [2], [3], communication performance of the phase-modulated FMCW signal has received much less attention.

Establishing a communication link between two FMCW RadCom systems requires detection of the RadCom signal at the receiver and synchronization of the receiver to the transmitting system. Diverse error sources, such as the limited accuracy of reference clocks on the transmitter and the receiver side and random delay on the echo signal due to the distance between the systems, make establishing a communication link challenging. It should be noted that these errors can be estimated and corrected, but first the presence of the RadCom signal has to be detected by the receiver and an initial estimate of the delay mismatch has to be obtained. The

reduced sampling rate at the FMCW radar receiver, which is one of the benefits of the stretch processing, limits the maximum mismatch between time references of the RadCom transmitter and the receiver. Beyond this maximum mismatch, the RadCom receiver is unable to sample the transmitted signal.

The contribution of this paper towards realization of PC-FMCW based RadCom systems is the experimental demonstration of the RadCom operation by a pair of PC-FMCW radars. Potential capability of transmitting and receiving RadCom signals by a pair of PC-FMCW radars with GPS-based synchronization is experimentally demonstrated for the first time. Using the same experiment setup, the mechanisms that may de-synchronize the RadCom systems are investigated. Results indicate that even external references such as GPS clocks have limited accuracy that may not be enough to recover the communication content. Moreover, the timing mismatch between internal clocks of RadCom systems may accumulate to result in a complete loss of the signal at the receiver. Another contribution of this paper is a novel signal detection technique that also provides the initial estimate of the timing mismatch between RadCom systems. Based on the initial delay mismatch estimate, the receiver can align its timing so that the mismatch between time references of the RadCom systems is reduced below the maximum delay imposed by the stretch processing.

The problem description is detailed in Section II, where the FMCW RadCom system is introduced and the necessity for the initial estimation of the timing mismatch is explained. Synchronisation experiments are described in Section III. The effect of various error sources are investigated and the capability to transmit, receive and decode FMCW radar signals is demonstrated. A novel synchronization approach, which is based on a detection scheme for FMCW RadCom signals based on sampling a constant frequency band is proposed and investigated in Section IV.

II. FMCW RADCOM SIGNAL DESCRIPTION

The phase-coded-FMCW (PC-FMCW) receiver is depicted in Fig. 1, where the communication payload modulates the phase of the FMCW signal through the phase term $\psi(t)$. The signal model and the radar receiver operation is investigated in [1], [4]. For the problem description at hand, which is the synchronization of a RadCom transmitter and receiver, a pilot

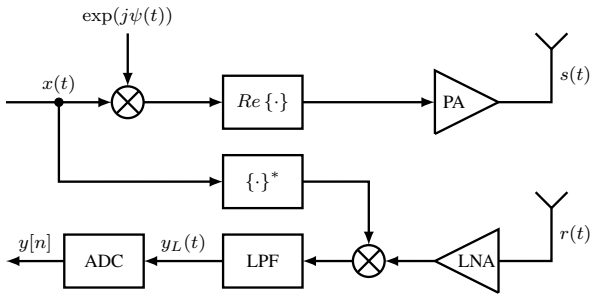


Fig. 1. Transceiver structure under consideration.

signal with no communication payload is assumed. The effect of the timing mismatch is equivalent to time of flight in case of an radar application and will therefore be referred to as τ . The received FMCW signal is written in exponential form for convenience. A detailed analysis of FMCW signal is presented in [5]. Considering a delay of τ at the received signal $r(t)$ with respect to the time reference at the transceiver, the received signal at the output of the low-pass filter can be written as

$$y_L(t) = \exp \left\{ j2\pi \left[-f_c\tau + \frac{\alpha}{2}\tau^2 - \alpha\tau t \right] \right\}. \quad (1)$$

Equation (1) consists of phase terms that solely depend on the carrier frequency f_c , delay τ and the beat frequency term that depends on both the slope of the frequency sweep α and the delay τ . The presence of the low-pass filter imposes a strict condition on the sampling of the signal after stretch processing; the beat frequency has to be lower than the cut-off frequency f_{co} of the low-pass filter. The limitation on the beat frequency translates to a maximum delay term:

$$\tau_{\max} = f_{co}/\alpha. \quad (2)$$

This signal model forms the basis of the system level synchronization proposed in Section IV. Before that, an assessment of the performance of synchronization based on external timing references is obtained through a set of experiments.

III. EXPERIMENTAL DEMONSTRATION OF COMMUNICATION BETWEEN PC-FMCW RADARS

In this section, an experimental setup for the transmission of information through FMCW radars is discussed. This setup has been realized with the aid of two automotive radar modules as well as two different brands automotive-grade GPS devices as shown in Fig. 2. The two radar modules are capable to perform a 180 degrees phase shift in their waveform during chirp transmission. This functionality has been exploited to create a binary symmetric channel between them on top of the LFM waveform used for sensing (see details at [6]). One of the main challenges in this implementation for communication has been to synchronize the two radar devices. Synchronization is necessary due to the intrinsic nature of an FMCW radar receiver. The waveform acquired after sampling at the receiver is obtained by mixing a locally generated waveform with the signal received by the antenna as illustrated in Fig. 1. Due

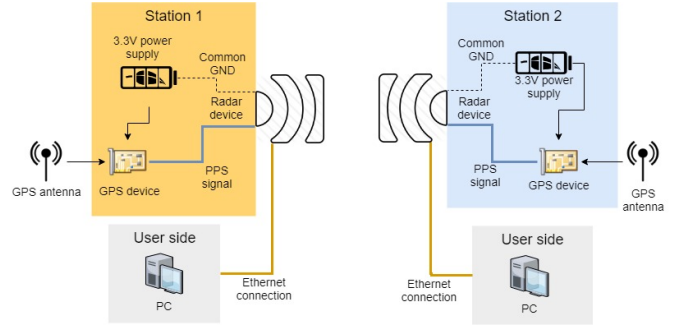


Fig. 2. Experimental setup illustration of a basic automotive radar RadCom system for joint sensing and communication.

to the finite bandwidth of analog mixing circuits, in the case of two unsynchronized radars, the receiver end would filter out the received signal and furthermore lose the information (Explicitly, any time delay bigger than (2) will cause desynchronization.). In this setup, synchronization has been achieved using the pulse per second (PPS) signal from two GPS modules which reset the relative time between two radar systems for each radar frame.

A. The Experimental Setup, Results and Waveform Evaluation

The radar modules (NXP TEF810X /S32R274 chipset) are positioned such that their antennas facing each other. Each one of them is connected to one GPS module. For illustration purpose, the transmitted data is set to a random BPSK code, which is generated on the host PC and then sent to the transmitting radar by TCP over an Ethernet connection.

The two radars are synchronized through the PPS signal generated by GPS. This is a square wave with a period of 1 second and a rising edge synchronized with the satellite signal. The two automotive-grade GPS devices come from two different manufacturers but mount the same Ublox Neo-7N chipset which can provide a PPS signal with a precision of 60ns (Experiments show a difference up to 800ns between the two GPS devices).

A beat signal in time domain for a single received pulse, containing 4-bit of random code, is illustrated in Fig. 3. The communication information can be extracted by computing the second derivative of the phase of the low-pass filtered received signal $y_L(t)$, which is illustrated in Fig. 4. As seen from the figure, a peak is created for each phase change which can be easily extracted by a simple threshold, under the assumption that the signal-to-noise ratio (SNR) available for communication is high. This assumption is reasonable for those transmitter-receiver distances that fall within the radar range. In this specific example, the 4 bit code can be extracted as either [0101] or [1010]. To address this ambiguity, we always code the first pulse of a frame with [0000] so we can keep track of the phase changes to solve the ambiguity on following pulses.

In the host system, one can perfectly decode the received signal (since the transmit code is known) and achieve range-Doppler information of the targets in the vicinity of the radar

which is out of the scope of this paper (interested readers can check [4], [6]).

B. Practical issues

Even though we managed to synchronize both radar systems for communication and demonstrate an initial success, there are some challenges that need to be addressed to realise reliable RadCom systems. During the course of experiments, we observed that there are different sources of error which may lead to desynchronization of the communication system, such as

- accuracy of GPS clock as well as PPS signal,
- accuracy of internal clocks of radar microcontroller unit (MCU) which controls the timing of phase changes during transmission,
- speed of the platforms (Doppler shift, out of the scope of this study),
- and the time of flight between the transmitter and the receiver.

It should be noted that these errors can be estimated and corrected. For instance, Fig. 5 illustrates the estimated synchronization error within a frame, which can be corrected in the next frames. Even though we reset the relative time to reduce the synchronization errors by using the PPS signal for

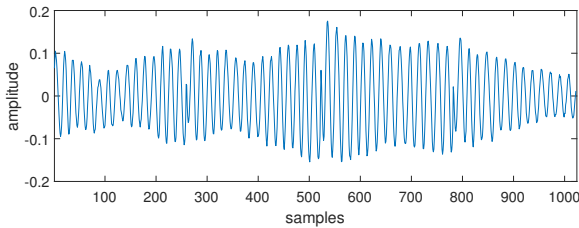


Fig. 3. Example of a received pulse.

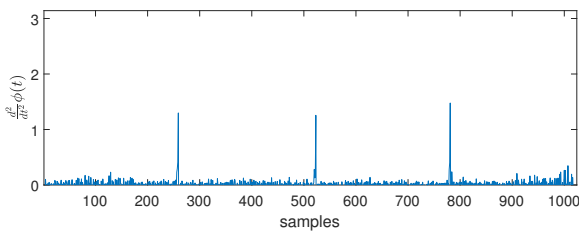


Fig. 4. Extraction of the phase code. Each peak represents a phase change.

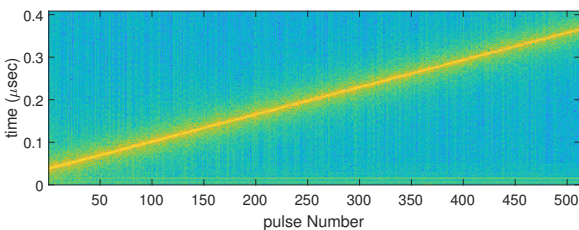


Fig. 5. Synchronization error between two radar boards versus slow-time (with in a single frame). Relative time resets for each frame, any delay bigger than (2) will cause de-synchronization.

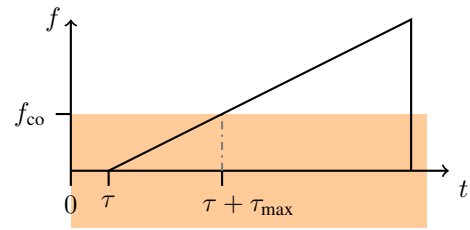


Fig. 6. Demodulation with constant frequency: Only the part of the signal which lies in the orange shaded strip is present in the baseband.

each frame, there are still synchronization errors. Moreover, the receiver may altogether fail to detect and synchronize with the transmitted signal if the delay is too long, as explained in Section II. Detection of the FMCW RadCom signals for initial synchronization (coarse alignment) will be explained in the next section.

IV. FMCW RADCOM SIGNAL DETECTION

Synchronization of a FMCW RadCom receiver to a transmitter starts with the detection of the signal at the receiver and proceeds with the estimation of discrepancies in the time and frequency references of the receiver. To establish a communication link between a transmitter-receiver pair, parameters of the waveform that carries the communication must be common on both the transmitter and the receiver. However, time and frequency references on both sides are inevitably mismatched and estimation of this mismatch at the receiver side is necessary before the communication content can be recovered.

The effect of time delay described in Section II indicates that for the detection of an incoming communication signal, the delay τ has to be bounded to keep the beat frequency below the cut-off frequency of the low-pass filter. However, bounding the delay term requires an additional means of synchronization. Another alternative is to change the reference signal so that the communications signal is partially sampled, which may allow the detection of the communication signal and estimation of the delay parameter τ . The stretch processing implemented in the transceiver structure in Fig. 1 must allow to set the the sweep slope to $\alpha = 0$, which corresponds to a constant carrier frequency f_c . Indicating the constant frequency reference signal phase by $\phi_0(t) = 2\pi f_c t$, then the stretch processing output in (1) can be rewritten as

$$y_L(t) = \begin{cases} \exp \left\{ j2\pi \left(\frac{\alpha}{2} (t - \tau)^2 - f_c \tau \right) \right\}, & t \in [\tau, \tau + \tau_{\max}] \\ 0, & \text{otherwise.} \end{cases} \quad (3)$$

It should be noted that the effect of a low-pass filter is to limit the frequency span of the frequency sweep at baseband that can be sampled by the receiver. The duration of the baseband sweep after sampling by the receiver is equal to the maximum delay term τ_{\max} in (2). The model of the received signal in (3) indicates that the task at hand consists of detection of the

presence of a communication signal with the delay parameter τ .

The detection is based on the sampled baseband signal for which we assume for the sake of simplicity that one of the sampling instants coincide with the beginning of the baseband chirp, i.e. $i \cdot f_s = \tau$ with $i \in \mathbb{Z}$. Thus, the sampled baseband signal can then be expressed as

$$y[n] = \sqrt{\frac{E}{N}} \exp \left\{ j \left(\pi \alpha \left(\frac{n}{f_s} \right)^2 - \Theta \right) \right\}, \quad (4)$$

where $n = 0, 1, \dots, N-1$, $\Theta = 2\pi f_c \cdot \tau$ is a constant phase term, and E is the energy of the received sampled baseband signal. Depending on f_s and τ_{\max} , $N = \lfloor \tau_{\max} \cdot f_s \rfloor$ samples are collected per chirp. N can be found in the range from a few samples up to tens of samples, depending on the radar parameters used. This makes the system fundamentally different from regular communications system where the signal can be acquired for an arbitrary time. At the front-end, additive white Gaussian noise (AWGN) is added to the received signal. Therefore, detection of the signal leads to a binary hypothesis test with the hypotheses:

$$\mathcal{H}_0 : u[n] = \nu[n], \quad \text{noise only} \quad (5)$$

$$\mathcal{H}_1 : u[n] = y[n] + \nu[n], \quad \text{signal plus noise.} \quad (6)$$

where the noise samples are assumed to be i.i.d. zero mean complex Gaussian noise, i.e. $\nu[n] \sim \mathcal{CN}(0, \sigma^2)$ with known variance σ^2 .

A. Energy Detection

The simplest approach of detecting the signal is by means of the received energy and therefore by an energy detector. Using an energy detector eliminates the necessity to know the waveform parameters. Communication between two RadCom systems requires the waveform parameters to be aligned, a mode of operation can be assumed where the RadCom systems are allowed to operate with different waveform parameters and the receiver aligns with the transmitter upon detecting the signal. The output of an energy detector is given as

$$r = \sum_{n=1}^N |u[n]|^2. \quad (7)$$

which is a random variable R . Since $|\nu[n]|^2 = \Re^2(\nu[n]) + \Im^2(\nu[n])$ and $\Re(\nu[n])$ and $\Im(\nu[n])$ are independent and identically distributed (i.i.d) zero mean Gaussian distributed with variance $\sigma_i^2 = \sigma^2/2$ is R under hypothesis \mathcal{H}_0 a sum of the squares of $N_f = 2 \cdot N$ Gaussian random variables. This distribution is known as generalized χ^2 -distribution with N_f degrees of freedom [7, p. 45]. The probability density function (pdf) of R is given as:

$$p_R(r|\mathcal{H}_0) = \begin{cases} \frac{r^{N_f/2-1}}{\sigma^{N_f} 2^{N_f/2} \Gamma(N_f/2)} \exp\left(-\frac{r}{2\sigma_i^2}\right), & r > 0 \\ 0, & r \leq 0, \end{cases} \quad (8)$$

where $\Gamma(\cdot)$ denotes the gamma function.

Under hypothesis \mathcal{H}_1 , i.e. the presence of a signal, R is distributed according to a generalized non-central χ^2 -distribution [7, p. 46]. The pdf under \mathcal{H}_1 is therefore:

$$p_R(r|\mathcal{H}_1) = \begin{cases} \frac{1}{2\sigma_i^2} \left(\frac{r}{s^2}\right)^{\frac{(N_f-2)}{4}} \exp\left(-\frac{s^2+r}{2\sigma_i^2}\right) \\ \cdot I_{\frac{N_f}{2}-1}\left(\sqrt{r}\frac{s}{\sigma_i^2}\right), & r > 0 \\ 0, & r \leq 0, \end{cases} \quad (9)$$

with N_f degrees of freedom and $s^2 = E$.

B. Matched Filter Detection

Since the transmitted waveform is known at the receiver, a matched filter can be applied. The causal matched filter is given as:

$$h[n] = \frac{1}{\sqrt{N}} \exp \left\{ -j\pi\alpha \left(\frac{(N-1)-n}{f_s} \right)^2 \right\}. \quad (10)$$

The matched filter is normalized to unit energy and the output of it is given as:

$$z = r[n] * h[n] \quad (11)$$

where $*$ denotes the convolution operator. Due to the unknown phase Θ , the output of the matched filter is fed into a square law device in order to make a decision. Under \mathcal{H}_0 is the output of the matched filter a linear combination of Gaussian random variables, which is again Gaussian and since the matched filter is normalized to unit energy is $Z \sim \mathcal{CN}(0, \sigma^2)$. The squared magnitude of z obeys a generalized χ^2 -distributions given in (8) with two degrees of freedom which is equivalent to an exponential distribution. Thus, $|Z|^2 = R \sim \text{Exp}(\lambda = 1/(2\sigma_i^2))$ with pdf:

$$p_R(r|\mathcal{H}_0) = \begin{cases} \lambda \exp(-\lambda \cdot r), & r \geq 0 \\ 0, & r < 0. \end{cases} \quad (12)$$

Under hypothesis \mathcal{H}_1 , the received signal is a sum of a chirp and the AWG noise. Due to the fact that the convolution operator is a linear operator the output of the matched filter can be written as

$$z = (y[n] + \nu[n]) * h[n]. \quad (13)$$

The convolution of the matched filter with the signal $y[n]$ results in:

$$y[n] * h[n] = \sqrt{E} \exp(j\Theta), \quad (14)$$

while the convolution with the noise is equivalent to z under hypothesis \mathcal{H}_0 . Thus, real and imaginary part are non-zero mean Gaussian random variables where $\Re\{z\} \sim \mathcal{N}(\sqrt{E} \cos(\Theta), \sigma_i^2)$ and $\Im\{z\} \sim \mathcal{N}(\sqrt{E} \sin(\Theta), \sigma_i^2)$. The square magnitude $R = |Z|^2$ is distributed according to a non-central χ^2 distribution as given in (9) with two degrees of freedom and $s^2 = E$.

C. Receiver Operating Characteristic

The receiver decides based on the decision variable r for one of the two hypotheses. Therefore, it compares the output of the energy detector or the matched filter with the threshold:

$$r \underset{\mathcal{H}_0}{\overset{\mathcal{H}_1}{\geq}} \eta. \quad (15)$$

The threshold is typically chosen to target a certain false alarm probability $P_{fa}(\eta)$ which is given as:

$$P_{fa}(\eta) = \Pr(R > \eta | \mathcal{H}_0). \quad (16)$$

Based on definition (16), the false alarm probabilities for a given threshold η can be obtained from the cumulative distribution function of the corresponding detectors under \mathcal{H}_0 :

$$P_{fa}(\eta) = \begin{cases} \exp\left(-\frac{\eta}{2\sigma_i^2}\right) \sum_{k=0}^{N-1} \frac{1}{k!} \left(\frac{\eta}{2\sigma_i^2}\right)^k, & \text{Energy Detector} \\ \exp\left(-\frac{\eta}{2\sigma_i^2}\right), & \text{Matched Filter.} \end{cases} \quad (17)$$

After a threshold value η has been chosen, the probability of detection P_d can be computed which is the probability that the decision variable y exceeds the threshold under hypothesis \mathcal{H}_1 :

$$P_d(\eta) = \Pr(R > \eta | \mathcal{H}_1) \quad (18)$$

which can be expressed for both detectors by the generalized Marcum Q function:

$$P_d(\eta) = Q_N\left(\frac{s}{\sigma_i}, \frac{\sqrt{\eta}}{\sigma_i}\right). \quad (19)$$

The only difference between P_d of the output of the two detectors is the degree of freedom of the individual distributions. While the output of the energy detector has $2N$ degrees of freedom the matched filter detector only has two degrees of freedom.

The performance of the two detectors was evaluated in terms probability of detection for a fixed probability of false alarm and is shown in Fig. 7. Using a matched filter is clearly beneficial in terms of probability of detection which assumes known waveform parameters at the receiver.

V. CONCLUSIONS

With this paper, for the first time, we demonstrate real-time synchronization of automotive-grade mmWave radars for joint sensing and communication purposes. The experiments highlight the challenge of synchronizing two RadCom systems; even with the external timing references, the timing errors can accumulate and desynchronize the systems.

Two detection methods, which are based on matched filter and energy detection, have been proposed for detection of RadCom signals from a transmitter. The novelty of the proposed methods is its sensing the transmitted signal through listening in the environment at a fixed frequency instead of sweeping the frequency. When the signal parameters are known, the matched filter is utilized and this provides superior detection

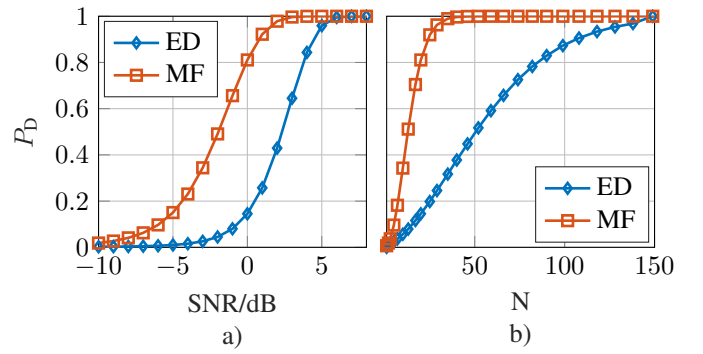


Fig. 7. Probability of detection P_D as a function of the SNR a) and number of samples b). In both examples, η was chosen to target a P_{fa} of 0.001. For a), N was set to 20 while in b) the SNR was fixed to 0 dB.

performance compared to energy detection. Utilization of the energy detector requires more SNR, however, it eliminates the necessity of knowing the transmitted signal parameters. Energy detection enables a greater degree of freedom when choosing the transmitted signal parameters.

Reliability of the synchronization in the long term (explicitly, keeping multiple units synchronized) as well as the assessment of sensing and communication performances are left for future work.

ACKNOWLEDGMENT

This project is supported by Netherlands Organisation for Scientific Research (NWO) under the contract ‘‘Integrated Cooperative Automated Vehicles’’ (i-CAVE). The authors wish to thank NXP Semiconductors N.V. for valuable discussions during their investigations.

REFERENCES

- [1] F. Lampel, R. F. Tigrek, A. Alvarado, and F. Willems, ‘‘A performance enhancement technique for a joint fmcw radcom system,’’ in *2019 16th European Radar Conference (EuRAD)*, Sep. 2019.
- [2] P. McCormick, C. Sahin, and J. M. Shannon Blunt, ‘‘FMCW implementation of phase-attached radar-communications (PARC),’’ in *Radar Conference (RadConf)*, Boston, USA, Apr. 2019.
- [3] H. Haderer, R. Feger, and A. Stelzer, ‘‘A comparison of phase-coded cw radar modulation schemes for integrated radar sensors,’’ in *2014 11th European Radar Conference*, Oct 2014, pp. 593–596.
- [4] F. Uysal, ‘‘Phase-coded FMCW automotive radar: System design and interference mitigation,’’ *submitted to IEEE Transactions on Vehicular Technology*, 2019.
- [5] A. G. Stove, ‘‘Linear FMCW radar techniques,’’ *IEE Proceedings F - Radar and Signal Processing*, vol. 139, no. 5, pp. 343–350, 1992.
- [6] F. Uysal and S. Orru, ‘‘Phase-coded FMCW automotive radar: Application and challenges,’’ in *preparation to Proc. IEEE Int. Radar Conf.*, Apr 2020.
- [7] J. Proakis and M. Salehi, *Digital Communications*. McGraw-Hill, 2008.